

COMMUNICATION

# Direct evidence for the participation of oxygen vacancies in CO oxidation over ceria supported gold catalysts using *operando* Raman spectroscopy

Marno Lohrenscheit, and Christian Hess\*

**Abstract:** Supported gold catalysts are highly active for a variety of reactions including low-temperature CO oxidation. It has been shown that reducible support materials, e.g. ceria or titania, may significantly alter the catalytic performance. However, the current understanding of the CO oxidation mechanism of such gold catalysts is still incomplete as important details such as the activation of oxygen or the role of oxygen vacancies are unknown. To elucidate the role of the ceria support during room-temperature CO oxidation we have employed *operando* Raman spectroscopy by simultaneously recording Raman spectra of the catalyst and gas-phase FT-IR spectra. Our results give first *direct* spectroscopic evidence for the participation of oxygen vacancies in the CO oxidation over ceria supported gold, thus underlining the crucial role of the support material for a detailed understanding of the mode of operation of supported gold catalysts.

Nano-sized gold particles dispersed on metal oxide supports are highly active for various reactions such as low-temperature CO oxidation, preferential CO oxidation and (reverse) water gas-shift.<sup>[1-6]</sup> While there has been considerable progress in the field, a detailed mechanistic understanding of the mode of operation of these catalysts is still missing. It is generally accepted in the literature that (i) the gold-support interface perimeter acts as the active site (ii) the oxide support strongly influences the catalytic properties (iii) the gold particle size plays an important role for catalytic activity.<sup>[7-10]</sup> Furthermore, it has been shown that the characteristics of reducible support materials such as ceria may significantly alter the catalytic performance.<sup>[11]</sup> Regarding the mechanism of CO oxidation over ceria supported gold, important details such as the activation of oxygen as well as the role of oxygen vacancies are still unknown. Oxygen activation may proceed (i) without participation of oxygen vacancies (ii) via vacancy-stabilized oxygen intermediates or (iii) via direct participation of lattice oxygen. Previous Raman work focused on  $F_{2g}$  phonon softening and the role of ceria bulk defects.<sup>[12]</sup> The stabilization of oxygen on one- and two-electron defect sites and the involvement of such species in CO oxidation has been proposed previously based on Raman spectra recorded before and after reaction.<sup>[13]</sup> Based on theoretical studies on ceria supported gold nanoparticles the participation of oxygen vacancies in CO oxidation has been proposed.<sup>[14]</sup> In this contribution, we present the first *direct* spectroscopic evidence for the participation of oxygen vacancies in CO oxidation over ceria supported gold catalysts (Au/ceria) by simultaneously recording

Raman spectra of the catalyst and gas-phase FT-IR spectra during reaction (*operando* Raman spectroscopy) and relating the dynamical behaviour of catalyst surface species with catalytic activity.

Figure 1 depicts the temporal evolution of the CO oxidation activity over 0.5 wt% Au/ceria at 25 °C as monitored by FT-IR gas phase spectroscopy (for details on the sample preparation and characterization see Experimental Section and Supporting Information Figure S1). As shown at the top, the gas feed was cycled between Ar/O<sub>2</sub> (3:1) and Ar/CO/O<sub>2</sub> (25:1:5) at a total flow rate of 100 ml/min. The CO conversions were determined as 9.8% and 6.1% at the maximum and the end of first Ar/CO/O<sub>2</sub> run, respectively. The bottom of Fig. 1 shows an expanded view of the activity in the first Ar/CO/O<sub>2</sub> run. A comparison of the gas phase signals reveals an initially slower response of the CO<sub>2</sub> signal indicating an activation period of the CO oxidation reaction in agreement with recent studies.<sup>[15]</sup> In the course of the reaction, the activity drops slowly after reaching its maximum after ca. 10 min. As a reason for the deactivation the formation of surface carbonates has been proposed **on the basis of DRIFTS**.<sup>[15]</sup>

Figure 2 depicts *operando* Raman spectra of 0.5 wt% Au/ceria taken during switching between non-reactive (Ar/O<sub>2</sub>) and reactive (Ar/CO/O<sub>2</sub>) conditions as indicated on the top of Fig. 1. The Raman spectra were recorded with a fibre optic probe using 532 nm laser excitation (for details on the *operando* setup see Experimental Section).<sup>[16]</sup> The Raman spectra of Au/ceria are dominated by a strong band at 463 cm<sup>-1</sup> due to the  $F_{2g}$  mode in cubic fluorite. Smaller bands appear at 255, ~590 (shoulder), 830 (several contributions) and 1172 cm<sup>-1</sup>, that have been assigned to bulk ceria, bulk defects in ceria, peroxide and second-order Raman scattering in ceria, respectively (see Supporting Information Figure S2).<sup>[17-19]</sup>

The top of Fig. 2 focuses on spectral changes in the peroxide range. The peroxide band around 840 cm<sup>-1</sup> results from adsorption of molecular oxygen on two-electron surface defect sites.<sup>[18]</sup> Close inspection of the band prior reaction (spectrum (1)) shows that the band is composed of (at least) three contributions located at 832, 847 and 881 cm<sup>-1</sup>, which have previously been assigned to peroxides adsorbed on defect sites with increasing degree of aggregation, respectively.<sup>[18]</sup> Upon switching from non-reactive to reactive conditions, the intensity of the peroxide band increases (spectrum (2)). Switching back to oxygen results in a further increase (spectrum (3)), while in Ar/CO/O<sub>2</sub> feed the intensity of the peroxide signal drops back to its original level in Ar/CO/O<sub>2</sub> (spectrum (4)). The observed behaviour during switching between non-reactive and reactive conditions is summarized on the bottom of Fig. 2 showing difference spectra of the peroxide signal for successive conditions. While the first exposure to reaction conditions leads to a strong increase of peroxide intensity attributed to catalyst rearrangement (e.g. catalyst reduction), subsequent switching results in reversible changes in peroxide intensities with higher overall peroxide concentrations under non-reactive conditions. This behaviour indicates that reactive peroxide species, particularly those corresponding to the features at 847 and 881 cm<sup>-1</sup>, are consumed during CO oxidation and replenished under oxygen flow. Other

[a] Marno Lohrenscheit, Prof. Dr. Christian Hess  
Eduard-Zintl-Institut für Anorganische und Physikalische Chemie  
Technische Universität Darmstadt  
Alarich-Weiss-Str. 8  
64287 Darmstadt (Germany)  
E-mail: hess@pc.chemie.tu-darmstadt.de

Supporting information for this article is given via a link at the end of the document.

peroxide features at 789 and 870  $\text{cm}^{-1}$  show the opposite behaviour suggesting their stabilization upon exposure to Ar/CO/O<sub>2</sub>. Regarding the 789  $\text{cm}^{-1}$  Raman feature, experiments in Ar/CO feed, which lead to a strong increase of the Raman intensity at 789  $\text{cm}^{-1}$ , are indicative of a stabilization by adsorbed CO.

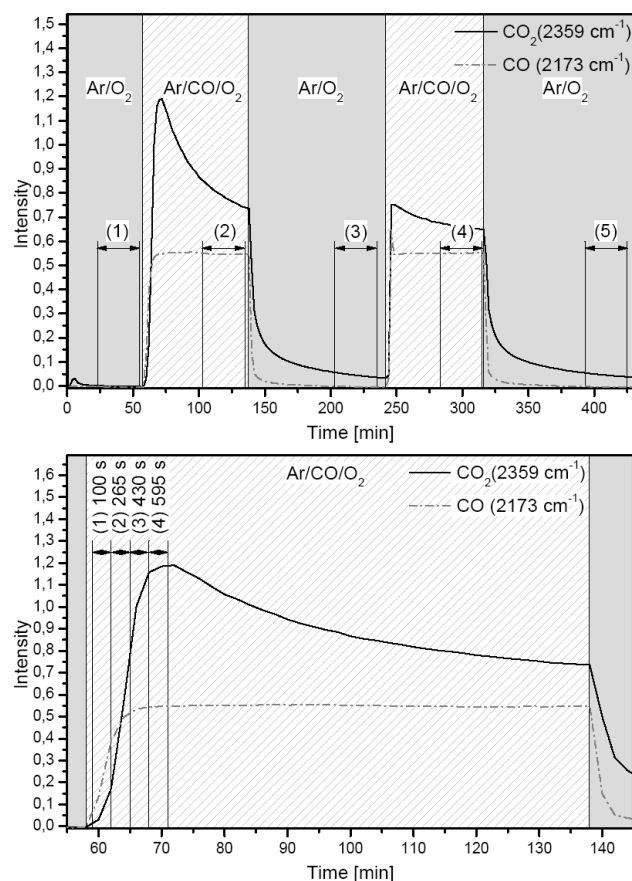


**Figure 1.** Top: Temporal evolution of the CO oxidation activity over 0.5 wt% Au/ceria at 25 °C as monitored by FT-IR gas phase spectroscopy. The gas feed was cycled between Ar/O<sub>2</sub> (3:1) and Ar/CO/O<sub>2</sub> (25:1:5) at a total flow rate of 100 ml/min. Bottom: Expanded view of the activity in the first Ar/CO/O<sub>2</sub> run. Arrows indicate start and end of *operando* Raman experiments.

To test this hypothesis, the dynamical behavior of the peroxide species was examined by time-dependent *operando* Raman spectroscopy during the onset of the CO oxidation reaction (see Fig. 1, bottom). Figure 3 shows the temporal evolution of spectral changes in the peroxide range. No other dynamics in the spectra was observed. In each panel, two subsequently recorded Raman spectra are depicted together with the corresponding difference spectrum. The resulting sequence of difference spectra clearly shows that initially formed peroxide species at 847 and 881  $\text{cm}^{-1}$  are continuously consumed during reaction, whereas the species at 830  $\text{cm}^{-1}$  does not undergo any significant changes under dynamical conditions. As the peroxide bands result from oxygen adsorption on two-electron defect sites, their consumption gives clear evidence for the participation of oxygen vacancies in the CO oxidation over Au/ceria at room temperature.

To gain insight into the nature of the peroxide features, *operando* Raman spectra were recorded during CO oxidation over bare

ceria (see Supporting Information, Figure S3). In the peroxide range, spectra are dominated by the 831  $\text{cm}^{-1}$  feature with a minor contribution from the 847  $\text{cm}^{-1}$  feature. In contrast to Au/ceria, the 847  $\text{cm}^{-1}$  did not show any dynamics in case of bare ceria. From this behaviour we conclude that the peroxide species giving rise to the feature at 881  $\text{cm}^{-1}$ , that is only observed in the presence of gold, are located directly at the gold-ceria interface, whereas 847  $\text{cm}^{-1}$ -related peroxide species may be associated with ceria defects (e.g. in the vicinity of the gold-ceria interface).

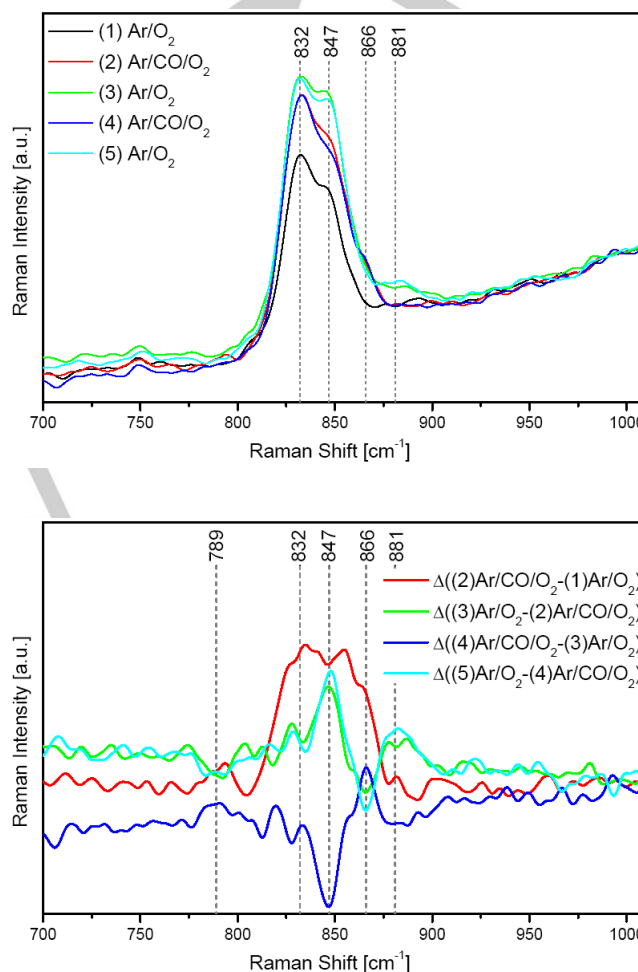


**Figure 2.** *Operando* Raman spectra of 0.5 wt% Au/ceria taken during cycling between Ar/O<sub>2</sub> (3:1) and Ar/CO/O<sub>2</sub> (25:1:5). Spectra were normalized to the intensity at 990  $\text{cm}^{-1}$ . Top: expanded view of the peroxide range. Bottom: difference spectra for successive conditions.

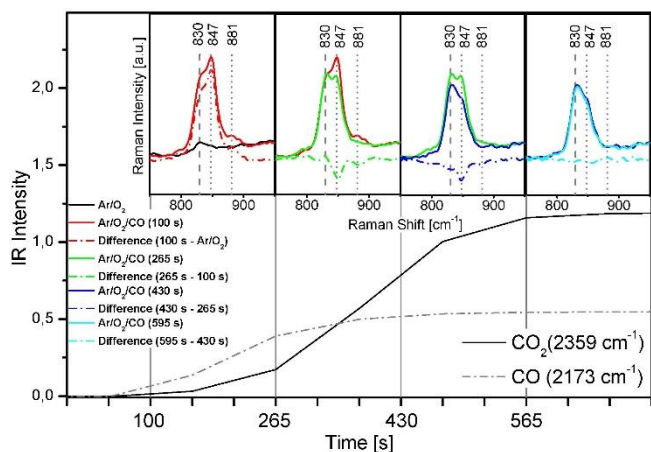


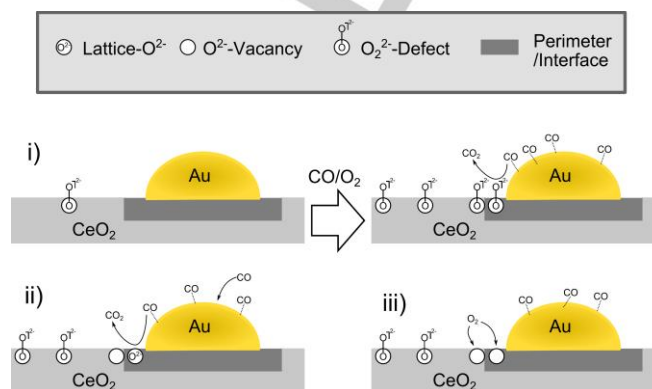
**Figure 3.** *Operando* Raman spectra of the peroxide range of 0.5 wt% Au/ceria during the onset of the CO oxidation reaction recorded during the intervals indicated in Fig. 1. Each panel shows two subsequently recorded Raman spectra together with the corresponding difference spectrum.

Based on our findings we propose the following processes to take place during room temperature CO oxidation over Au/ceria (see Scheme 1): (i) Gas-phase oxygen molecules adsorb onto two-electron defects sites at the gold-ceria interface and are consumed by reaction with adsorbed CO (ii) Lattice oxygen is consumed by reaction with adsorbed CO. (iii) Oxygen vacancies are replenished by gas-phase oxygen.

The proposed processes are consistent with theoretical results on the CO oxidation mechanism on ceria supported gold nanoparticles.<sup>[14]</sup> According to this DFT study oxygen vacancies near the gold-ceria interface are suggested as anchoring sites for O<sub>2</sub>, that subsequently reacts with Au-CO to form CO<sub>2</sub> (second half of the Mars-van-Krevelen (MvK) mechanism). Such an oxygen vacancy-mediated O<sub>2</sub> activation significantly reduces the barrier for oxygen activation. In the course of the reaction, the second oxygen atom heals the vacancy. In agreement with the first half of the MvK mechanism, lattice oxygen is then consumed in a reaction with CO leading again to the formation of oxygen vacancies. Considering the activation barrier for the removal of lattice oxygen the formed CO<sub>2</sub> is expected to stay on the surface e.g. as carbonate species (see above). The formed oxygen vacancies can be replenished by diffusion of peroxide species from the vicinity of the gold-ceria interface perimeter (species at 847 cm<sup>-1</sup>) to the gold-ceria interface perimeter (species at 881 cm<sup>-1</sup>). The simultaneous disappearance of both peroxide features indicates fast diffusion of peroxide species (as compared to our temporal resolution). The higher intensity of the 847 cm<sup>-1</sup> feature originates from the higher abundance of oxygen vacancy sites in the vicinity compared to the interface. It should be mentioned that other proposed CO oxidation mechanisms such as CO oxidation by coadsorbed O<sub>2</sub> (Langmuir-Hinshelwood mechanism) or CO oxidation by O<sub>2</sub> bound to Au-Ce<sup>3+</sup> sites are not excluded by our results. Previous studies have demonstrated the importance of oxygen vacancies in CO oxidation also for other ceria-based catalysts.<sup>[20,21]</sup> In case of ceria supported platinum catalysts, active Ce<sup>3+</sup> species were detected during reaction using resonant X-ray emission spectroscopy.<sup>[20]</sup> Doping ceria with praseodymium increases the concentration of oxygen vacancies, which in turn was shown to enhance the reactivity.<sup>[21]</sup>

Summarizing, by using *operando* Raman spectroscopy we provide *direct* spectroscopic evidence for the participation of oxygen vacancies in the CO oxidation over ceria supported gold

catalysts at room temperature. Our results underline the crucial role of the support material for a detailed understanding of the mode of operation of supported gold catalysts.



**Scheme 1.** Proposed processes during room temperature CO oxidation over Au/ceria.

## Experimental Section

The nano-crystalline ceria support was prepared by decomposition of cerium nitrate at 600 °C. Gold was loaded onto ceria by deposition precipitation of HAuCl<sub>4</sub> using NaOH as described elsewhere.<sup>[5]</sup> The catalyst was dried overnight at 110 °C and subsequently calcined for 12 h at 500 °C. The total Au content of the final catalyst was determined as 0.5 wt% using chemical analysis. The Au/ceria catalyst exhibited a BET surface area of 56 m<sup>2</sup>/g showing <1% variation due to reaction. Transmission electron microscopy (TEM) showed the presence of 3 nm-sized Au particles. Analysis of X-ray photoelectron spectra revealed that the majority of gold particles is in a metallic state (Au<sup>0</sup>) and only about 6% is in an oxidized state (Au<sup>+</sup>) (see Supporting Information, Figure S1)

For Raman experiments a frequency-doubled Nd:YAG laser (Cobolt AB) operated at 532 nm and a transmission spectrometer (Kaiser Optical, HL5R) equipped with a CCD detector (Andor) were employed. The resolution of this instrument is 5 cm<sup>-1</sup>; however, the wavelength reproducibility is better than 0.5 cm<sup>-1</sup>. The laser was operated at a power level of 2 mW as measured with a power meter (Ophir) at the position of the sample. Raman spectra were collected in a 180° backscattering geometry using a fibre probe (Kaiser Optical, IO-12L-VS). *Operando* Raman experiments were performed by using a setup described in detail elsewhere,<sup>[16]</sup> which was extended by a FT-IR spectrometer (Bruker Vertex 70, DLaTGS detector) to analyse the outlet gases of the *in situ* cell. The CO oxidation activity was monitored based on the CO and CO<sub>2</sub> gas-phase signals at 2173 cm<sup>-1</sup> and 2369 cm<sup>-1</sup>, respectively.

## Acknowledgements

The authors thank Christian Schilling for help with the activity measurements, Xing Huang (Fritz-Haber-Institut) and Marc

Willinger (Fritz-Haber-Institut) for performing TEM experiments as well as Karl Kopp for technical support.

**Keywords:** gold • ceria • CO oxidation • Raman spectroscopy • operando

- [1] M. Haruta, T. Kobayashi, H. Sano, N. Yamada, *Chem. Phys. Lett.* **1987**, *16*, 405-408.
- [2] M. Valden, X. Lai, D. W. Goodman, *Science* **1998**, *281*, 1647-1650.
- [3] Q. Fu, H. Saltsburg, M. Flytzani-Stephanopoulos, *Science* **2003**, *301*, 935-938.
- [4] X. W. Xie, Y. Li, Z. Q. Liu, M. Haruta, W. J. Shen, *Nature* **2009**, *458*, 746-749.
- [5] J. Fonseca, S. Royer, N. D. Duprez, F. Epron, *Appl. Catal. B* **2012**, *128*, 10-20.
- [6] G. Hutchings in *Nanostructured Catalysts: Selective Oxidations*, Vol. 8 (Eds.: C. Hess, R. Schlögl), RSC, Cambridge, **2011**, pp. 193-213.
- [7] M. Haruta, *CATTECH* **2002**, *6*, 102-105.
- [8] I. X. Green, W. J. Tang, M. Neurock, J. T. Yates, *Science* **2011**, *333*, 736-739.
- [9] T. Takei, T. Akita, I. Nakamura, T. Fujitani, M. Okumura, R. Okzaki, J. Huang, T. Ishida, M. Haruta in *Advances in Catalysis*, Vol. 55 (Eds.: B. C. Gates, F. C. Jentoft), Elsevier, Amsterdam, **2012**, pp. 1-124.
- [10] D. Widmann, R. J. Behm, *Angew. Chem. Int. Ed.* **2011**, *50*, 10241-10245.
- [11] M. M. Schubert, S. Hackenberg, A. C. van Veen, M. Muhler, V. Plzak, R. J. Behm, *J. Catal.* **2001**, *197*, 113-122.
- [12] Y. Lee, G. He, A. J. Akey, R. Si, M. Flytzani-Stephanopoulos, I. P. Herman, *J. Am. Chem. Soc.* **2011**, *133*, 12952-12955.
- [13] J. Guzman, S. Carrettin, A. Corma, *J. Am. Chem. Soc.* **2005**, *127*, 3286-3287.
- [14] H. Y. Kim, H. M. Lee, G. Henkelman, *J. Am. Chem. Soc.* **2012**, *134*, 1560-1570.
- [15] S. Zhang, X.-S. Li, B. Chen, X. Zhu, C. Shi, A.-M. Zhu, *ACS Catal.* **2014**, *4*, 3481-3489.
- [16] C. T. Nottbohm, C. Hess, *Catal. Comm.* **2012**, *22*, 39-42.
- [17] W. H. Weber, K. C. Hass, J. R. McBride, *Phys. Rev. B* **1993**, *48*, 178-185.
- [18] V. V. Pushkarev, V. I. Kovalchuk, J. L. d'Itri, *J. Phys. Chem. B* **2004**, *108*, 5341-5348.
- [19] Z. Wu, M. Li, J. Howe, H.M. Meyer, S.H. Overbury, *Langmuir* **2010**, *26*, 16595-16606.
- [20] R. Kopelent, J. A. van Bokhoven, J. Szlachetko, J. Edebeli, C. Paun, M. Nachttegaal, O. V. Safonova, *Angew. Chem. Int. Ed.* **2015**, *54*, 1-5.
- [21] Z.-Y. Pu, X.-S. Liu, A.-P. Jia, Y.-L. Xie, J.-Q. Lu, M.-F. Luo, *J. Phys. Chem. C* **2008**, *112*, 15045-15051.

## COMMUNICATION

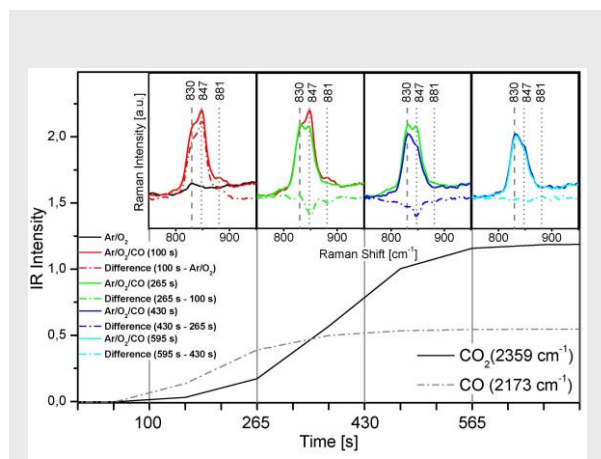
Entry for the Table of Contents (Please choose one layout)

## COMMUNICATION

Marno Lohrenscheit, Christian Hess\*

Page No. – Page No.

Direct evidence for the participation of oxygen vacancies in CO oxidation over ceria supported gold catalysts using *operando* Raman spectroscopy



By using *operando* Raman spectroscopy we provide *direct* spectroscopic evidence for the participation of oxygen vacancies in the CO oxidation over ceria supported gold catalysts at room temperature. Our results underline the crucial role of the support material for a detailed understanding of the mode of operation of supported gold catalysts.

Supporting Information

[Click here to download Supporting Information: Supporting Information.pdf](#)